

3<sup>rd</sup> International Conference on Biomedical Engineering and Technology

## The 3D Eyeball FEA Model with Needle Rotation

Jing Wu<sup>a,\*</sup>, M. A. Nasser<sup>b</sup>, M. Eder<sup>c</sup>, M. Azqueta Gavaldon<sup>c</sup>, C. P. Lohmann<sup>d</sup> and  
Alois Knoll<sup>c</sup>

<sup>a</sup> Nanjing University of science & technology, Nanjing, China

<sup>b</sup> Graduate School of Information Science in Health, Technische Universität München, Germany

<sup>c</sup> Department of Robotics and Embedded System, Technische Universität München, Germany

<sup>d</sup> Augenklinik Rechts der Isar, Technische Universität München, Germany

---

### Abstract

Definition of the force and torque boundaries during ophthalmic operations is a vital step towards design and development of robotic solutions for eye surgery. This paper describes the development of an eyeball FEA model. Unlike other eyeball FEA studies, this 3D eyeball model contains all three layers of the inner eye: retina, choroid and sclera. Furthermore the model includes six extra ocular muscles. The intraocular rotation of a needle tool using a trocar during the surgery was also considered in this study. Although variables such as the thickness of the layers and the property of the orbits and the muscles are unique for every individual, the model was developed by introducing some assumptions and constraints for an average eye. However by changing few parameters a modified model suitable for individuals can be generated. The model gives the stress distribution when the needle rotates inside the eyeball. The results of this study will give a numerical understanding of the forces which are needed for ophthalmic operation.

© 2013 The Authors. Published by Elsevier B.V.

Selection and peer-review under responsibility of Asia-Pacific Chemical, Biological & Environmental Engineering Society.

*Keywords:* Eyeball FEA model, Eye model, Robot assisted eye surgery, biomechanics

---

### 1. Introduction

Globally eye surgeons have to deal with scenarios that request a lot of skills in terms of high precision manipulation of surgical devices. Today robotic solutions have attracted research groups as a promising tool

---

\* Corresponding author. Tel.: +8613951741250.

E-mail address: [rose.pianist.219@163.com](mailto:rose.pianist.219@163.com).

to assist surgeons in such high-precision tasks. The objective of ophthalmic surgical devices is to assist the surgeon for manipulating the tool inside the eye and on the surface of the retina. The robots have to control the force and movement of the needle during the vitreo-retinal surgery as well as filter the tremors. Safety issues should be considered as highest priorities for controlling the robot. So it is important to figure out the stress and strain distribution when the needle is inserted into the eyeball.

Schutte et al. [1] developed an eyeball FEA model containing 3D orbital biomechanical interactions, such as the 4 recut muscles, the eyeball, the orbital fat and also the interactions between these tissues. Z. Yiyi [4] [7] generated an FEA eyeball- model with 6 muscles, and validated the eyeball movement caused by the outside forces. E. Uchio [6] developed a simulation of an eyeball, which contained cornea, sclera, lens and vitreous layers; this study determined the physical and mechanical foreign bodies' impact conditions caused by intraocular foreign body (IOFB) injuries, they used Blunt shaped missiles to evaluate the surface of the cornea or sclera. But there was no muscles attached. Richard E. Norman [11] developed a 2D model of the human sclera, but their model contained only sclera and the optic nerve head. Qi Wei [3] presented a 3D biomechanical model of the oculo motor plant; they got the simulated results of the eyeball gaze position and trajectories, but the 4 resulting muscles were modeled as prismatic joints.

A 3D FEA model of an eyeball and the attached muscles is modeled in this paper. The rotation of the needle will lead to a movement of the orbit, and then of the muscles. The orbit will also rotate and influence the needle in turn. By analyzing the stress distribution and the displacement of the attached muscle, the needed and maximum allowed force and displacement of the needle is defined. This data is used to design relevant control approaches for robotic devices in the future.

## 2. Geometric Model

### 2.1. Eyeball model

The most common way to obtain a eyeball geometric model is by deriving the geometry of the orbital structures from MRI scans. Previous studies used this method to observe the geometric model [1][2]. K. Duška [9] was able to create a 3D model of a human head in Matlab using MRI DICOM data. E. N. Richard [10] employed Amira to create a meshed volume of the ocular anatomy from segmented MRI images.

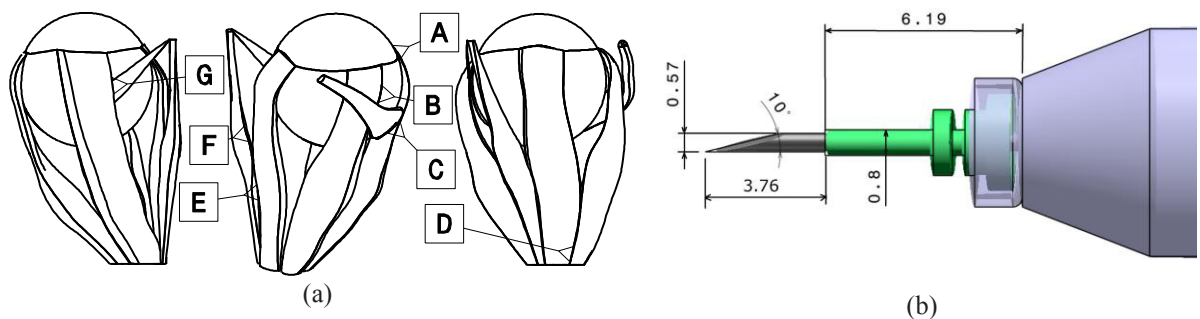


Fig. 1. (a) Geometric model of the Eye, A. Eye ball, B. IR, C. IO, D. LR, E. MR, F. So, G. SR, (b) Needle geometric model, 23 gauge trocar.

The geometric model used in this paper is given by S. Schutte [1], from Delft University of Technology. This geometric model was derived from frontal MRI scans. A 3D region-growing algorithm was used to accurately segment the anatomical structures of interests, such as the orbit and six extra ocular muscles:

Superior rectus (SR), Inferior rectus (IR), Lateral rectus (LR), Medial rectus (MR), Superior oblique (SO) and Inferior oblique (IO) (Fig. 1. (a)).

## 2.2. Needle model

The most common tools which are used in current ophthalmic surgeries are 23 gauge tools with cross-section diameter of 0.574mm. As a representation of one of these tools, a needle is modeled in this study (see Fig.1.(b) is a simple trocar system tool). Here the needle is assumed to be a rigid body.

## 3. Meshed Model and Boundary Conditions

In order to create the finite elements, the geometry was imported to the finite-element preprocessor software in IGES format. First, the insertion point of the needle was subtracted from the eyeball surface with a Boolean method. The resulting shell then contains 3089 elements (160 tri elements and 2929 quad elements). Furthermore, the muscles were subdivided into tetrahedral elements with an average edge length of 1mm, resulting in a total number of 16405 muscle elements. The needle was considered to be a rigid body and it was meshed into 20 rigid elements (R3D4 element type). The resulting eyeball FE model is shown in Fig. 2.(a).

The four rectus muscles of the eye and the superior oblique muscle are fixed in one end to the back of the eye. The same way, the inferior oblique is attached to the lower front of the nasal orbital wall [4] in this model. This anatomical layout was modeled and additionally, all of the six muscles were connected to the eyeball at the insertion nodes.

The eyeball surface was coupled with the central point (0, 0, 0). Considering the natural movement of the eye, this central point was constrained to have solely 3 DOF and perform only rotational movements.

The nodes on the eyeball in contact with the needle were assumed to be tied on the surface of the needle.

The intraocular pressure (IOP) of 2kPa, uniformly distributed on the inner surface of the eyeball, was also taken into consideration within the simulations.

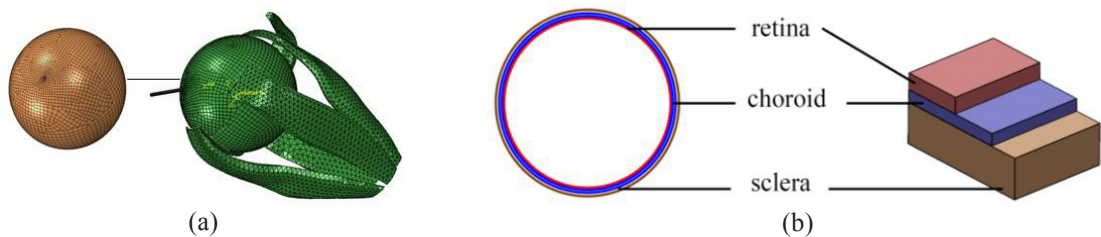


Fig. 2. (a) Eyeball FE model, (b) Three layers of the eyeball.

## 4. Material Properties

The ocular organ is made of several tissues. There are three layers inside the eyeball, sclera, choroid and retina. According to [11] [9] [8], the thicknesses of these three layers are not constant throughout the whole surface. The most inner layer, the retina, is only present in 72% of the orbit, more precisely in the distal part of the eyeball. However, considering of the geometric model and the effect of the tissues during the surgery, the thicknesses of the layers are assumed to be constants, and there is no other tissue inside the eyeball, as shown in Fig. 2.(b) The ocular organ is made of several tissues. There are three layers inside the eyeball, sclera, choroid and retina. According to [11] [9] [8], the thicknesses of these three layers are not constant throughout the whole surface. The most inner layer, the retina, is only present in 72% of the orbit, more

precisely in the distal part of the eyeball. However, considering of the geometric model and the effect of the tissues during the surgery, the thicknesses of the layers are assumed to be constants, and there is no other tissue inside the eyeball, as shown in Fig. 2.(b).

The properties of the tissue are assumed to be linear and elastic as it can be seen in TABLE I.

The extra ocular muscles are hyper elastic, and they have similar material properties to silicone rubber [11]. The detailed data of the rubber mechanical properties can be found in [5].

The surgical needle is made of steel. In contact with the ocular soft tissue, when penetrating it, the deformation of the tool is almost none, especially when compared to that of the eyeball. Both the stress and the deformation can be thus ignored. With the aim of reducing computation costs, the needle is modeled as a rigid body.

It should be mentioned that all these values were found in these papers. Different paper, due to inconstancy of layer thickness, represent different vales., e.g, the mean thickness of retina is 100~230 $\mu\text{m}$  in [12], but 249mm in [13], it depends on the age and the healthy situation of the sample person, and the position we want to put the needle in. It is too complex to define all the thickness of the retina in different position, so we have to make these assumptions to reduce our calculations.

Table I. Eyeball's Property

| Property                    | Sclera      | Choroid    | Retina     |
|-----------------------------|-------------|------------|------------|
| E (Young's modulus)         | 2900kPa [9] | 220kPa [9] | 20 kPa [9] |
| $\nu$ (Poisson's ratio)     | 0.4         | 0.49       | 0.49 [8]   |
| Thickness ( $\mu\text{m}$ ) | 700 [11]    | 80 [9]     | 200        |

## 5. Results

Shutte et al. [1] simulated the eyeball with the rotation of 10.5° as a result of external forces exerted by a tool, See Gomez-Perez et al. work [2] simulated the eyeball rotating 7~9.1° due to the muscle movement. In this paper, the needle was assumed to rotate 10° around the pinpoint around different axes. 4 different kinds of rotations were simulated as Table II shows:

Table II. Four kinds of needle rotation

| Case   | Boundary condition                   |
|--------|--------------------------------------|
| Case 1 | $x=10^\circ, y=0^\circ, z=0^\circ$   |
| Case 2 | $x=0^\circ, y=10^\circ, z=0^\circ$   |
| Case 3 | $x=0^\circ, y=0^\circ, z=10^\circ$   |
| Case 4 | $x=10^\circ, y=10^\circ, z=10^\circ$ |

### 5.1. Case 1

In the first scenario that is simulated, the needle pinned to the entry point rotates solely around the x axis. The movement of the needle is thus constrained to one degree of freedom.

The von Mises stress on sclera and retina is shown in Fig.3. The largest stress on sclera is 131.6MPa, and on the retina it is 2.2MPa. The highest deformation on the tissue is 1.64mm, located on the superior oblique muscle as it can be seen in Fig.3. Accordingly, when the needle rotates around the x axis, the fraction of the sclera near the needle will bear the greatest pressure and the stress on retina will be subsequently lower. The SO muscle will deform largely in order to keep the eyeball steady.

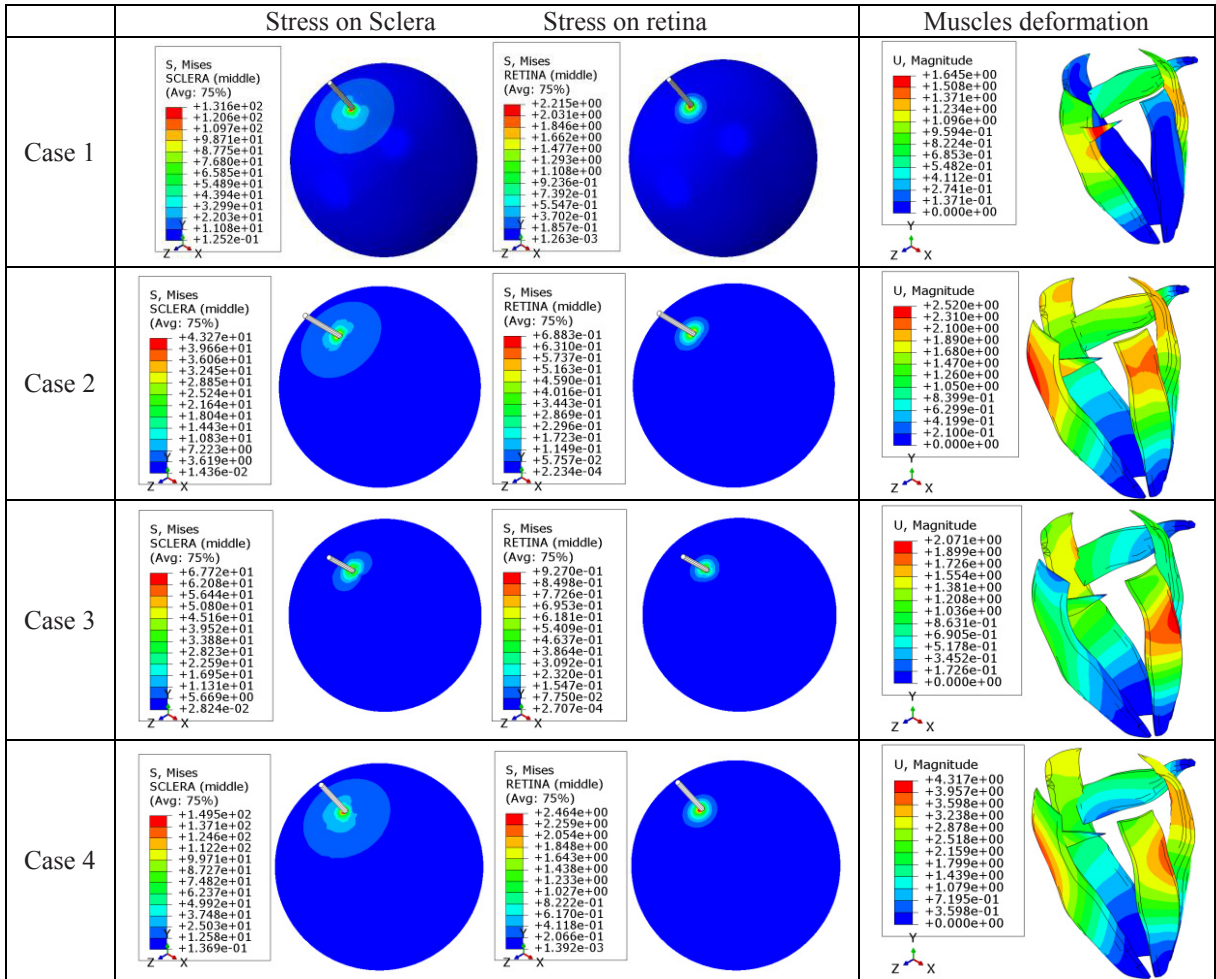


Fig. 3. Stresses and deformations of the eyeball and muscles for different cases

5.2. Case 2

Another setting where the needle rotates 10° around the pinpoint on the y axis is modeled. As in the previous case, the other degrees of freedom are fixed. The von Mises stress on sclera and retina is illustrated in Fig.3. The biggest stress on sclera is 43.27MPa, on the retina it is 0.68MPa. The most substantial deformation on the tissue is 2.52mm, being the SR muscle the one standing this maximum distortion (Fig. 3).

5.3. Case 3

In the case of a 10° rotation of the needle around pinpoint exclusively on z axis with the other degrees of freedom constrained, the von Mises stress on sclera and retina is shown in Fig. 3. The maximum stresses in sclera and retina are found to be 67.72 MPa and 0.93 MPa respectively. In this case the MR muscle undergoes

the highest deformation, concretely 2.07mm (Fig. 3).

#### 5.4. Case 4

A movement with higher degrees of freedom is modeled as well. In this case, the needle rotates  $10^\circ$  around pinpoint on x, y and z axis. It can be observed higher maximum stresses on both sclera and retina compared with the previous cases: 149 MPa and 2.46 MPa. The maximum deformation, beard by the SR muscle in this case is also higher: 4.37mm (Fig 4).

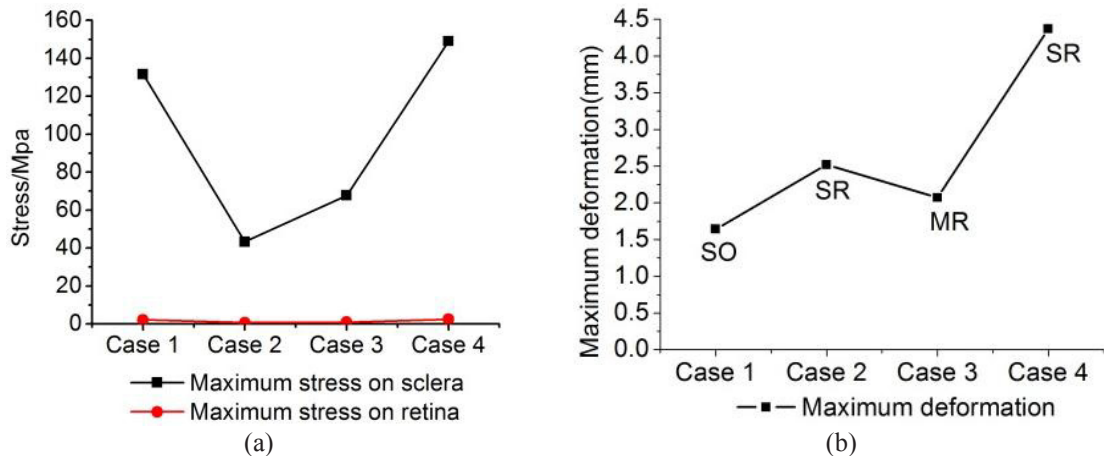


Fig. 4. (a) Max stress on orbit in 4 cases, (b) Max deformation and location of the muscles in 4 cases

This noticeable rise in the stresses can be explained by the fact that the needle rotates about three axes, and consequently, the total displacement is maximum. As shown in Fig.4.(a), the sclera bears a greater stress than the retina. This is due to the property of the materials; more specifically due to the fact the sclera has a larger Young's modulus than the retina. The force on the eyeball layers in case 1 is 0.67% bigger than in case 2, and it surpasses by 49% the one in case 3. This may also be due to the location of the needle and the angle of the needle with respect to the eyeball.

As Fig.4.(b) shows, different rotation directions produce maximum deformation of the muscles located in different muscles. In this respect, the length, thickness and also the position of the muscle cannot be ignored in the biomechanical analysis of the orbit.

## 6. Conclusion

An eyeball FEA model with 3 layers together with the attached muscles was built in this paper. This model also includes the needle penetrating the three layers of the inner eye, which can simulate the rotation of the needle during an eye surgery well. The IOP was also considered in this analysis. The simulated results can give a better understanding of how the eyeball interacts with surgical devices by means of stress and strain distribution, the pressure on the surface of the eyeball and the displacement of the muscles, which can help in the design of a mechanical robot.

The sclera has a bigger Young's modulus than the retina. Taking this into account when the robot is programmed to assist in the eyeball surgery a much bigger force will be exerted in the sclera than in the retina

when the needle moves inside the orbit. Furthermore, as mentioned previously, when the needle rotates around the x axis, the orbit layers will bear more force than when the needle is rotating in other directions. The position of the muscle can also affect the stress distribution on the eyeball. Correspondingly, if the surgeon has knowledge prior to the operation about the precise force and deformation that the orbit organ can undergo, he can plan the surgery optimally.

Concerning future work some more detailed work could be done in order to overcome the limitations of the current assumptions. The thickness of the layers could be more relative; the aqueous fluid inside the orbit might be added to the FEA model; also friction between the eyeball and the needle might be considered. Moreover, the material properties of the ocular tissue should be validated with some empirical data.

## References

- [1] S. Sander, Sven P.W. van den Bedemb, Fred van Keulen, Frans C.T. van der Helma, J. S. Huibert, "A finite-element analysis model of orbital biomechanics". *Vision Research* vol. 46, 2006, pp. 1724–1731
- [2] M. Gomez-Perez, P. Young, V. Bui Xuan, "New tools for analyzing biomechanical problems". *ABAQUS Users' Conference*. 2007, pp. 1-9
- [3] W. Qi, S. Shinjiro, K. P.Dinesh, "Biomechanical Simulation of Human Eye Movement". *ISBMS'10 Proceedings of the 5th international conference on Biomedical Simulation*, 2010, pp. 108-118
- [4] Z. Yiyi, W. Guangzhil, D. Huil, J. Yonghon, "The Finite Element Model and Biomechanical Analysis of the Eyeball-Extraoculars". *Beijing Biomedical Engineering*. Vol. 25 No.3, 2006, pp. 228-230
- [5] Z. Zhuang, F. Zhang, S. Qin, X.C. You, X.G. Yu, Q.C. Mou, M. Xu and R. Bai, *Abaqus nonlinear finite element analysis example*, J.Z. Lv, CN: Science Press, 2005, ch.4.
- [6] E. Uchio, S. Ohno, J. Kudoh, K. Aoki, L.T. Kisielwicz, "Simulation model of an eyeball based on finite element analysis on a supercomputer". *Br J Ophthalmol*. Vol. 83(10), 1999, pp. 1106-11.
- [7] Z. Yiyi, W. Guangzhi, D. Hui, J. Yonghong, "Finite Element Modeling and Biomechanical Analysis of Eyeball and Extraocular Muscles", *Engineering in Medicine and Biology 27th Annual Conference*, 2005 Sep, pp. 1-4
- [8] V. Manjunath, M. Taha, J. G. Fujimoto, J. S. Duker, "Choroidal Thickness in Normal Eyes Measured Using Cirrus HD Optical Coherence Tomography". *American Journal of Ophthalmology*, Vol. 150, 2010, pp.325-329
- [9] K. Duška, J. Milorad, R. Branimir, "3D Visualisation of MRI images using matlab". *Journal of Automatic Control*, University of Belgrade, Vol. 16, 2006, pp. 1-3
- [10] E. N. Richard, G. F. John, A. S. Ian, M.K. R. Sophie, T. Inka, C. R. Ethier, "Finite element modeling of the human sclera: Influence on optic nerve head biomechanics and connections with glaucoma". *Experimental Eye Research*. Vol. 93, 2011, pp. 4-12
- [11] Z. A. Mohd, S. Lee, C. Cho, "Hyperelastic Muscle Simulation". *Key Engineering Materials*. Vol. 345-346, 2007, pp. 1241-1244
- [12] I. L. JONES!, M. WARNER!, J. D. STEVENS2, "Mathematical modelling of the elastic properties of retina: a determination of young's modulus". *Eye*. Vol. 6, 1992, pp. 556-559
- [13] B Alamouti, J Funk, "Retinal thickness decreases with age: an OCT study". *Br J Ophthalmol*. Vol. 87, 2003;87:899–90